AIMS Mathematics, 11(3): 6231–6250.
DOI: 10.3934/math.2026257
Received: 30 September 2025
Revised: 27 February 2026
Accepted: 03 March 2026
Published: 11 March 2026

https://www.aimspress.com/journal/Math

Research article

Web and tableau representations of rank two cluster variables for Gr (5,9)

Rui Zhi Tang and Jin Xing Zhao*

School of Mathematical Sciences, Inner Mongolia University, Hohhot, China; Email: zhjxing@imu.edu.cn (Zhao), tangrzh01@gmail.com (Tang)

* **Correspondence:** Email: zhjxing@imu.edu.cn.

Abstract: Tymoczko and Russell provide a bijection between semi-standard tableaux of rectangular shapes and sl_r-webs when $r \leq 3$. Due to Chang, Duan, Fraser, and Li, cluster variables in the Grassmannian cluster algebra correspond to certain semi-standard tableaux of rectangular shapes. When $r = 2$ or $r = 3$, the cluster variables in the Grassmannian cluster algebra can be represented both by tableaux and webs. Recently, Elkin, Musiker, and Wright refined the twist map, providing a method to connect webs and cluster polynomials through the compatibility defined by Lam in 2015, thereby also connecting cluster variables and webs. In this paper, we study the webs corresponding to rank 2 Plücker polynomials, particularly cluster variables in the Grassmannian cluster algebra $\mathbb{C}[\mathrm{Gr}(5,9)]$. Additionally, we examine the webs corresponding to rank 2 cluster variables in $\mathrm{Gr}(5,9)$, and we find 11 distinct webs (up to dihedral translation) arising from these variables. Consequently, we propose a conjecture that for all cluster variables the webs obtained through the diagram method and the compatibility method coincide.

Keywords: grassmannian, cluster algebra; sl_r-webs; tableaux
Mathematics Subject Classification (2020): Primary 05E10, 13F60; Secondary 14M15

1. Introduction

Cluster algebras, invented by Fomin and Zelevinsky in [1], have become a pivotal topic in algebraic combinatorics due to their extensive connections across various mathematical domains. The foundational work on the cluster structure on Grassmannians, $\mathrm{Gr}(k,n)$, was initiated by Scott in [2], who not only introduced these structures but also demonstrated that their cluster algebras were of finite type under specific conditions. Further combinatorial explorations of these algebras were conducted by Postnikov in [3], who introduced plabic graphs as the primary tool for examining these structures. Postnikov also devised a boundary measurement map, connecting Plücker coordinates with dimers on plabic graphs, effectively parameterizing the Grassmannian as a projective variety. The understanding

of this map was deepened by Talaska in [4], and later, the series of papers [5] by Muller and Speyer and [6] by Marsh and Scott elaborated on the Laurent expansions of Plücker coordinates under the twist map, initially established by Berenstein, Fomin and Zelevinsky in [7].

Building on Postnikov's description of $\mathrm{Gr}(k,n)$ via plabic graphs and dimers [3], Lam studied dimers on these graphs and introduced a compatibility condition between Plücker monomials and non-crossing matchings, expressing certain Plücker coordinates and cluster variables as sums of dimer weights [8]. More recently, Elkin, Musiker and Wright refined the twist map for quadratic and cubic cluster variables in $\mathrm{Gr}(3,n)$, expressing the twisted cluster variables as double and triple dimer partition functions on plabic graphs [9]. Their work provides additional motivation for studying the relationship between cluster variables and webs.

Conceptually, these results indicate that, once the web corresponding to a cluster variable is known, its image can be recovered under the twist map from suitable dimer partition functions on a plabic graph. However, using the method of compatibility requires enumerating all possible "irreducible webs", which is not a trivial task. In addition, in [10], (m,n)-diagrams were introduced by Westbury, and in [11, Section 7], cup diagrams were defined by Fung in the context of the Kazhdan–Lusztig basis. Tymoczko introduced the m-diagrams to give an explicit bijection between $3\times n$ standard Young tableaux and irreducible sl_3-webs in [12], and Russell extended this framework to semi-standard Young tableaux with mixed boundary conditions [13]. Since this paper deals exclusively with rank 2 cluster variables, it suffices to rely solely on the results of [11].

Actually, there is another bijection between sl_r-webs and Young tableaux called the web invariant, which was introduced by Kuperberg in [14] and was applied to cluster algebras by Fomin and Pylyavskyy in [15]. The irreducible webs studied by Westbury, Fung, Tymoczko, and Russell are precisely the dual diagrams of these web invariants. In [16], Fraser, Lam, and Le established a bijection between the Plücker coordinate ring $\mathbb{C}[\mathrm{Gr}(k,n)]$ and the dual of the tensor invariant space. Moreover, Fraser [17] and Gaetz et al. [18] respectively presented explicit algorithms for computing the quadratic dual canonical basis in $\mathbb{C}[\mathrm{Gr}(k,n)]$ and the dual canonical basis in $\mathbb{C}[\mathrm{Gr}(4,n)]$, together with the corresponding tensor invariants. In related work, Lam showed that, in degree two, the dual canonical basis of $\mathbb{C}[\mathrm{Gr}(k,n)]$ is given by web (Temperley–Lieb) immanants. In particular, every degree-two element of the homogeneous coordinate ring (and hence every degree-two cluster variable) can be expressed in terms of web immanants [19].

In this paper, to simplify the process of identifying the webs corresponding to the cluster variables described in [9], we study the 576 different rank 2 cluster variables in $\mathrm{Gr}(5,9)$ using the two distinct methodologies, the method of compatibility in [8] and the method of diagram in [11]. Specifically, the computational enumeration in [20] lists 576 rank 2 cluster variables in $\mathrm{Gr}(5,9)$; up to dihedral translations, we select 11 representatives, each of which corresponds to a distinct sl_2-web. Throughout this paper, we take this enumeration as input data for our computations, and we do not claim an independent proof of its completeness. The method of compatibility associates each cluster variable directly to an sl_2-web, whereas the method of diagram maps every semi-standard Young tableau to a non-crossing matching that forms a basis of sl_2-webs. Since Chang [21] provides an explicit algorithm, based on Kazhdan–Lusztig polynomials, that matches a semi-standard Young tableau with a polynomial in Plücker coordinates, we adopt this algorithm to link the two methods above and to compute the web associated with each cluster variable, namely the dual web of its web invariant. Our findings indicate that the methods of compatibility and diagram yield the same sl_2-web for any

given rank 2 cluster variable in Gr(5, 9). Building on the results of [9], which studied quadratic and cubic cluster variables in Gr(3, n), we therefore propose the following conjecture, stated precisely as Conjecture 4.7: For any cluster variable written as both a Young tableau and a polynomial, the corresponding webs from the method of diagram and compatibility are the same.

The organization of this paper is as follows: In Section 2, some necessary definitions, including cluster algebras, sl_2-webs and the character ch(T) are given. Then in Section 3, we detail the aforementioned two methods, which are called compatibility and cup diagram respectively. Section 4 applies these methodologies to explore the rank 2 cluster variables of Gr(5, n), focusing on the associated webs for Gr(5, 9). In Section 5, all rank 2 cluster variables (up to dihedral translation) in Gr(5, 9) appeared in [20] (totally 576 of them) and their corresponding webs are listed to prove the theorem in Section 4.3.

2. Preliminaries

For convenience, denote by $[n]$ the set $\{1, 2, \ldots, n\}$. For $1 \leq k \leq n$, denote by $\binom{[n]}{k}$ the set of all subsets with k elements in $[n]$.

2.1. Grassmannians

In this section, we briefly review the structure of the Grassmannian; see [22] for details.

The Grassmannian, denoted Gr(k, n), is the space of k-dimensional linear subspaces in $\mathbb{C}^n$. It can be parametrized by the Plücker embedding into projective space $\mathbb{P}^{\binom{n}{k}-1}$. Any point in Gr($k, n$), can be represented by a matrix $M \in \mathrm{Mat}_{k\times n}(\mathbb{C})$, and the embedding map is defined as follows: For any $J \in \binom{[n]}{k}$, there is a corresponding projective **Plücker coordinate** P_J, and at the point M, the value of $P_J(M)$ is defined as the minor of M using the column set J.

For any k and n, the set of Plücker coordinates satisfies some certain quadratic **Plücker relations**.

Example 2.1. *A general point $M \in$ Gr(k, n) is represented by a row-reduced matrix*

$$M = \begin{pmatrix} 1 & 0 & a & b \\ 0 & 1 & c & d \end{pmatrix} \quad a, b, c, d \in \mathbb{C}.$$

The Plücker coordinates are as follows:

$$\begin{array}{lll} P_{12} = 1, & P_{13} = c, & P_{14} = d, \\ P_{23} = -a, & P_{24} = -b, & P_{34} = ad - bc. \end{array}$$

These coordinates satisfy the algebraic relation $P_{24} \cdot P_{13} = P_{12} \cdot P_{34} + P_{23} \cdot P_{14}$.

The homogeneous coordinate ring of Gr(k, n), denoted $\mathbb{C}$[Gr(k, n)], is the coordinate ring of the affine cone over Gr(k, n). In [2], Scott showed that $\mathbb{C}$[Gr(k, n)] is a cluster algebra in the sense of [1].

2.2. sl_2-Webs

In this section, we review the definition of sl_r-webs. Kuperburg first introduced sl_3-webs in [14], which were studied further by [23] and [24], then settled for all r in [25] and connected to dimers in [16]. We will only need sl_2-webs, because they correspond to the rank 2 cluster variables.

Definition 1. *[16] Assume $k < n$. Fix an integer $r \geq 2$ and a sequence $\lambda = \{\lambda_1, \lambda_2, \ldots, \lambda_n\}$ with $0 \leq \lambda_i \leq r$ and $\lambda_1 + \lambda_2 + \ldots + \lambda_n = kr$. sl_r-**webs** are planar graphs in the disk with n boundary vertices $v_1, v_2, \ldots, v_n$ such that the degree of vertex v_i is exactly λ_i, and the degree of interior vertices is r.*

See [16] for details. In particular, if $r = 1$, the sl_1-webs are sets of boundary vertices, $\lambda_i \in \{0, 1\}$. Vertex v_i is included in the set if and only if $\lambda_i = 1$. If $r = 2$, the sl_2-webs are non-crossing matchings such that v_i is included in the matchings if and only if $\lambda_i = 1$, and v_i is a white boundary vertex if and only if $\lambda_i = 2$. These non-crossing matchings form the standard web basis for the space of sl_2-invariants for the diagonal action on the tensor product representation specified by the boundary type λ; see [16].

For convenience, unless dihedral translates are explicitly invoked, we label the boundary vertices of every sl_2-web considered in this paper $1, \ldots, n$ in clockwise order, starting from the topmost vertex.

2.3. Semi-standard Young tablueax and polynomials

In this section, we briefly review the Plücker character map introduced in [21]. We denote by $\mathrm{SSYT}(n, [m])$ the set of all semi-standard Young tableaux with at most n rows and entries in $[m]$, denote by S_k the symmetric group on k symbols, denote by $\ell(w)$ the coxeter length of $w \in S_k$, and denote by $w_0 \in S_k$ the longest permutation.

Definition 2. *[21, Definitions 3.4, 3.11] Let T be a single column Young tableau with n rows whose entries, read from top to bottom, are $t_1 < t_2 < \cdots < t_n$. The **gap weight** of T is defined as $t_n - t_1 - n + 1$. For a general Young tableau T,*

- *T has **small gaps** if every column of T has gap weight exactly 1.*
- *T is called **trivial** if every column of T has gap weight exactly 0.*

Given two Young tableaux T' and T'', form their disjoint union and then reorder the entries in each row in increasing order, the resulting Young tableau is denoted $T = T' \cup T''$. For two Young tableaux S and T, we write $S \sim T$ if there exists a trivial Young tableau T_0 such that $S = T \cup T_0$.

To translate a small-gap tableau into an explicit Plücker polynomial, we must record the order of its columns and then permute the corresponding column sets accordingly.

Definition 3. *[21, Definition 5.6] Let T be a small gaps tableau with r columns, with $i = (i_1 \leq \cdots \leq i_r)$ the first-row entries of the small-gaps tableau T, and $j = (j_1 \leq \cdots \leq j_r)$ the weakly increasing sequence obtained by sorting the multiset of missing entries of T, meaning the unique elements of $[i_1, i_1 + k], \ldots, [i_r, i_r + k]$ that do not appear in the corresponding columns of T. Both viewed as elements of $\mathbb{Z}^r$. For $u \in S_r$, define $P_{u;T}$ as follows. Provided $j_a \in [i_{u(a)}, i_{u(a)} + k]$ for all $a \in [r]$, define the tableau $\alpha(u; T)$ to be a rectangular Young tableau whose columns have content $[i_{u(a)}, i_{u(a)} + k] \backslash \{j_a\}$ for $a \in [r]$, and define $P_{u;T} = P_{\alpha(u;T)} \in \mathbb{C}[\mathrm{Gr}(k, n)]$ to be the corresponding standard monomial. On the other hand, if $j_a \notin [i_{u(a)}, i_{u(a)} + k]$ for some a, then the tableau $\alpha(u; T)$ is undefined and $P_{u;T} = 0$.*

Note that for some $u \in S_r$, $P_{u;T} = P_T$, denote $\mathcal{U}_T$ the set $\{u \in S_r : P_{u;T} = P_T\}$. Let w_T be the maximal length permutation in $\mathcal{U}_T$.

Theorem 2.2. *[21, Theorem 5.8] For $T \in SSYT(k,[n])$ with gap weight r, let $T' \sim T$ the small gaps tableau equivalent to T. Then*

$$ch(T') = \sum_{u \in S_r} (-1)^{\ell(uw_T)} p_{uw_0, w_T w_0}(1) P_{u;T'}$$

where $p_{\lambda,\mu}(t)$ is the Kazhdan-Lusztig polynomial. And if $T' = T \cup T_{triv}$, then $ch(T') = P_{T_{triv}} ch(T)$.

By this theorem, we relate the two methods introduced in Section 3 and examine the Plücker polynomials and Young tableaux of all cluster variables described in Section 5.

3. The method of compatibility and diagram

In this section, we will review two distinct methods for obtaining a diagram associated with a cluster variable. These are the method of compatibility introduced in [8,16], which associates a cluster variable with a diagram, and the method of cup-diagram introduced in [10, 11] , which associates a rectangular semi-standard Young tableau with a diagram.

3.1. Compatibility

Definition 4. *[8, Section 3.1] Let W be an sl_2-web with n boundary vertices $v_1, \ldots, v_n$. Suppose I and J are subsets of $[n]$ such that $|I| = |J| = k$. A monomial $P = P_I P_J$ and the non-crossing matching W are said to be **compatible** if and only if the labels of any two boundary vertices connected by an arc (excluding the boundary circle) belong to the sets $I \setminus J$ and $J \setminus I$, respectively. If $i \in I \cap J$, then the boundary vertex v_i is white and does not connect to any other boundary vertices.*

Indeed, an sl_2-web can be viewed as a non-crossing matching between the vertex sets $I \setminus J$ and $J \setminus I$. In our context, we generally take I and J to be the column index sets in a product of Plücker coordinates $P_I P_J$.

Let $\mathbb{C}[\mathrm{Gr}(k,n)]$ denote the homogeneous coordinate ring of the Grassmannian, and write $\mathbb{C}[\mathrm{Gr}(k,n)]_2$ for its degree-two homogeneous component. Following Lam's work on dimers, webs and positroids [8], one associates to each non-crossing matching on $[n]$ (equivalently, to each sl_2-web W with boundary vertices labelled in $[n]$) a degree-two polynomial

$$\mathrm{Imm}_W \in \mathbb{C}[\mathrm{Gr}(k,n)]_2,$$

called the web (or Temperley–Lieb) immanant corresponding to W. Thus the symbol Imm_W will always denote this polynomial attached to the web W.

For a pair (I, J) with $|I| = |J| = k$, let $C(I, J)$ be the set of all sl_2-webs W whose underlying non-crossing matching is compatible with (I, J) in the sense of the above definition. The key structural result we need can be stated as follows.

Theorem 3.1 ([8, Theorem 3.1])**.** *For any $I, J \subset [n]$ with $|I| = |J| = k$ we have*

$$P_I P_J = \sum_{W \in C(I,J)} \mathrm{Imm}_W,$$

where P_I and P_J are the Plücker coordinates on $\mathrm{Gr}(k,n)$.

In particular, the web immanants Imm_W span the degree-two component $\mathbb{C}[\mathrm{Gr}(k,n)]_2$, and any quadratic Plücker polynomial

$$P = \sum_i c_i P_{I_i} P_{J_i}, \quad c_i \in \mathbb{Z}$$

can be rewritten as an integer linear combination of web immanants by applying the above formula to each monomial $P_{I_i}P_{J_i}$ and then collecting terms. In this paper, the quadratic Plücker polynomials we study have coefficients $\mathrm{sgn}_i \in \{\pm 1\}$, but the same rewriting procedure applies verbatim to any integer linear combination of monomials $P_{I_i}P_{J_i}$.

Therefore, to apply the method of compatibility to a given quadratic Plücker polynomial P, one first enumerates all candidate sl_2-webs W, then uses Theorem 3.1 to compare the associated web immanants Imm_W with P in order to test compatibility, and finally identifies the webs whose immanants occur in the expansion of P as the webs compatible with P.

3.2. Cup diagrams

In [10], the definition of (m,n)-diagram was introduced, while in [11], a further definition of cup diagram was given, together with a bijection between cup diagrams and standard Young tableaux of two-row shape.

In this paper, we instead work with tableaux of *two-column shape*, in order to match the column-indexing convention for Plücker coordinates used in [21] via $ch(T)$. Accordingly, whenever we invoke the cup diagram, we apply it to the transpose $T^\top$ of our two-column tableau T.

Definition 5. *[11, Definition 7.1] Suppose we have the numbers 1 to n on a horizontal line, increasing to the right. Then an (n,p)-cup diagram consists of p cups on these numbers, where each cup connects two numbers, no two cups intersect each other, and no number is underneath a cup and yet not connected to any cup. The entire cup diagram must lie in one half-plane.*

Explicitly, let A be a standard Young tableau of shape τ. In our two-column convention, we start from a two-column tableau T and set $A = T^\top$. Read the entries $1, 2, \ldots, n$ from left to right along a horizontal line: open a cup at i whenever i lies in the bottom row of A, and close the most recently opened but unfinished cup at i whenever i lies in the top row; any endpoint left unmatched is kept blank (an "orphan"). This algorithm yields a bijection between two-row tableaux and (n,p)-cup diagrams.

For convenience, we also record the number of times each number from 1 to n appears in the tableau as a sequence, denoted by $\lambda = \{\lambda_1, \lambda_2, \ldots, \lambda_n\}$, where λ_i represents the frequency of occurrence of the number i in the Young tableau. Although it is an abuse of notation, the relationship between Young tableaux and webs that is discussed in this paper ensures that such usage does not lead to ambiguity.

Example 3.2. *Consider the quadratic cluster variable $X = P_{134}P_{256} - P_{156}P_{234}$ in the Grassmannian* $\mathrm{Gr}(3,6)$. *The standard Young tableau corresponding to the dual web of X is* $T = \begin{array}{|c|c|c|}\hline 1&2&4\\\hline 3&5&6\\\hline\end{array}$. *There are* 3 *arcs,* $\{1,6\}$, $\{2,3\}$, *and* $\{4,5\}$, *the diagram of T is the left of Figure 1. Afterwards, by connecting the ends of the lines, we obtain the sl_2-web corresponding to T.*

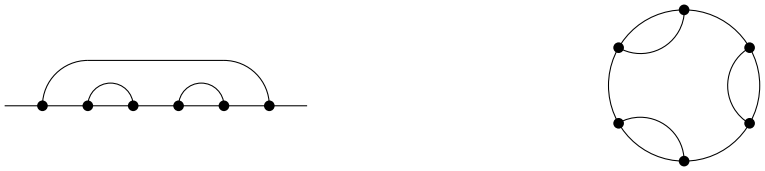

Figure 1. The cup diagram (left) and the sl_2-web (right) of T.

For a semi-standard Young tableau, in which the elements filled in the boxes of the Young diagram may include identical numbers, the elements in each column are strictly increasing. Consequently, identical numbers cannot appear in the same column. To convert this into a standard Young tableau, one can use the following method from [13]: For a number k that appears λ_k times (in fact, we just study when $\lambda_k \leq 2$), replace each occurrence of k with numbers from $1 + \sum_{i=1}^{k-1} \lambda_i$ to $\sum_{i=1}^{k} \lambda_i$, in sequence, according to the positions of the columns of the boxes from left to right.

After drawing the diagram corresponding to the standard Young tableau, it is necessary to translate it into the original semi-standard Young tableau.

The notion of a sink vertex is taken from [13], where it is formulated for general webs. In the rank 2 setting of this paper, this contraction only serves to undo the standardization step for repeated entries and it produces an isolated white boundary vertex.

Definition 6. *[13] In the process depicted in Figure 2, the resulting white boundary vertex is referred to as a* ***sink vertex****. This means that if two adjacent black boundary vertices are connected to the same white internal vertex, in certain cases, we can merge their corresponding boundary edges and consolidate these two black boundary vertices with the white internal vertex into a unique white boundary vertex.*

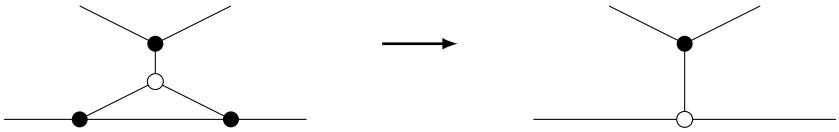

Figure 2. The procedure of contracting boundary edges to produce a sink vertex.

Using the concept of a sink vertex, we can contract the same numbers that were split during the conversion process from a semi-standard Young tableau to a standard Young tableau. This allows us to reconstruct the original numbers and obtain the diagram corresponding to the semi-standard Young tableau.

In this paper, we study solely rank 2 cluster variables, which correspond to sl_2-webs. Therefore, the sink vertices are actually isolated white vertices in the context of these webs.

For instance, Example 4.1 has a semi-standard Young tableau that can be transformed into a standard Young tableau using the above method, and then its corresponding web can be drawn.

In [12], a method is provided for mapping diagrams which consist exclusively of black boundary vertices to Young tableaux. Here, we keep the two-column tableau convention; equivalently, we apply the row-based description to the transpose $T^\top$ (a two-row tableau) and then interpret the result for T. As illustrated in Figure 3, for each face f in the diagram, label it according to the following rule: Choose a segment that connects f to the outer face without crossing the boundary line and with the

fewest number of edges crossed. The number of edges crossed is then used as the label for the face. Consequently, for a boundary vertex corresponding to a number, if the label of the face to its left is greater than that on its right, place it in the first row; if less, in the second row. Since each column in a Young tableau must strictly increase, this process results in a standard Young tableau.

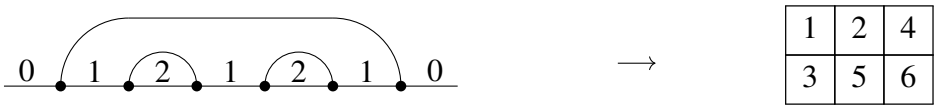

Figure 3. The cup diagram (left) and its corresponding standard Young tableau (right).

The web obtained by this method is precisely the diagram mentioned earlier, and the previously mentioned dual diagram can be produced by applying the same procedure to the transpose of the Young tableau. In what follows, to align with the earlier result on Compatibility, we will first take the transpose and then draw the diagram—that is, we will work with the dual diagrams.

4. Webs for quadratic differences

This section primarily establishes the relationship between webs and Young tableaux, starting with two examples that utilize the content of Section 3 to derive the same web using two different methods. Subsequently, it presents the webs corresponding to all rank 2 cluster variables in $\mathrm{Gr}(5, 9)$. Although Grassmannian $\mathrm{Gr}(5, 9) \cong \mathrm{Gr}(4, 9)$, we work with $\mathrm{Gr}(5, 9)$ because the natural map $\mathrm{Gr}(5, 8) \to \mathrm{Gr}(5, 9)$ induces a canonical cluster-subalgebra embedding, whereas the corresponding relationship between $\mathrm{Gr}(4, 9)$ and $\mathrm{Gr}(3, 8)$ is less transparent.

4.1. Enumeration of non-crossing webs

To study the compatibility between webs and cluster variables, we need to enumerate all candidate webs. For instance, from [16, Appendix], there are three types of sl_2-webs with 8 black boundary vertices (up to the dihedral translates), listed in Figure 4. By varying the position where a white boundary vertex is inserted, we obtain all non-crossing matchings with 8 black and 1 white boundary vertex in Figure 5.

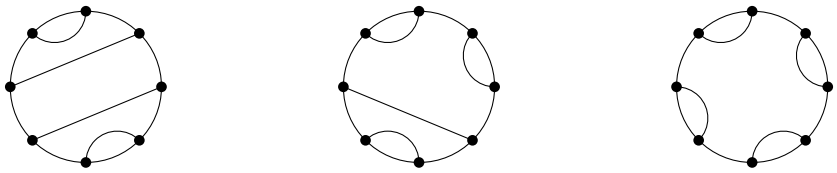

Figure 4. The enumeration of sl_2-webs with 8 black vertices.

We fix the white vertex at the top, that is $\lambda_1 = 2$, which allows us to enumerate 14 non-crossing matchings.

Similarly, we fix a white vertex at the top, and choose the other white vertex with the minimum possible index, that is, λ_1 and λ_i are the white boundary vertices with $2 \leq i \leq 5$. Then the 14 webs with 6 black vertices and 2 white are enumerated in Figure 6, which can also be obtained by inserting two distinct white boundary vertices into a web that originally has only six black boundary vertices.

For ease of use in Section 4.2 and 4.3, in Figure 6, a web and its reflections are considered identical, whereas in Figure 5, they are not treated as such.

We do not identify reflections in Figure 5, because in Example 4.1 we will refer to individual compatible webs term-by-term, and keeping mirror-distinct representatives makes it easier for the reader to locate each web unambiguously.

In fact, there exist sl_2-webs with 4 black and 3 white boundary vertices, as well as sl_2-webs with 2 black and 4 white boundary vertices; these webs correspond respectively to the Grassmannians $\mathbb{C}[\mathrm{Gr}(5,7)]$ and $\mathbb{C}[\mathrm{Gr}(5,6)]$. However, since $\mathrm{Gr}(5,7) \cong \mathrm{Gr}(2,7)$ and $\mathrm{Gr}(5,6) \cong \mathrm{Gr}(1,6)$, the associated cluster algebras contain no rank 2 cluster variables, so we do not discuss those cases here.

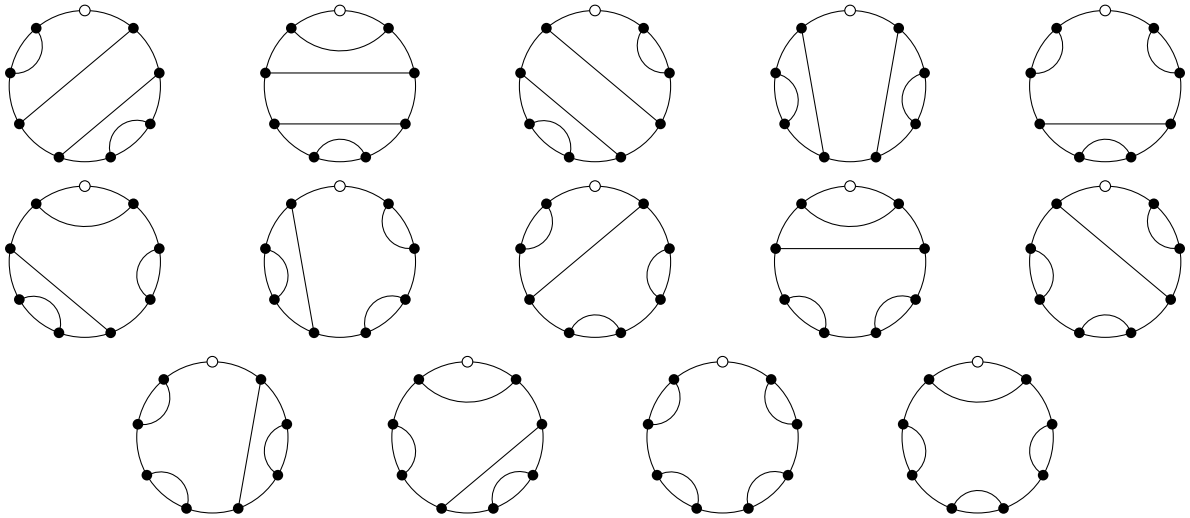

Figure 5. The enumeration of sl_2-webs with 8 black and 1 white vertex.

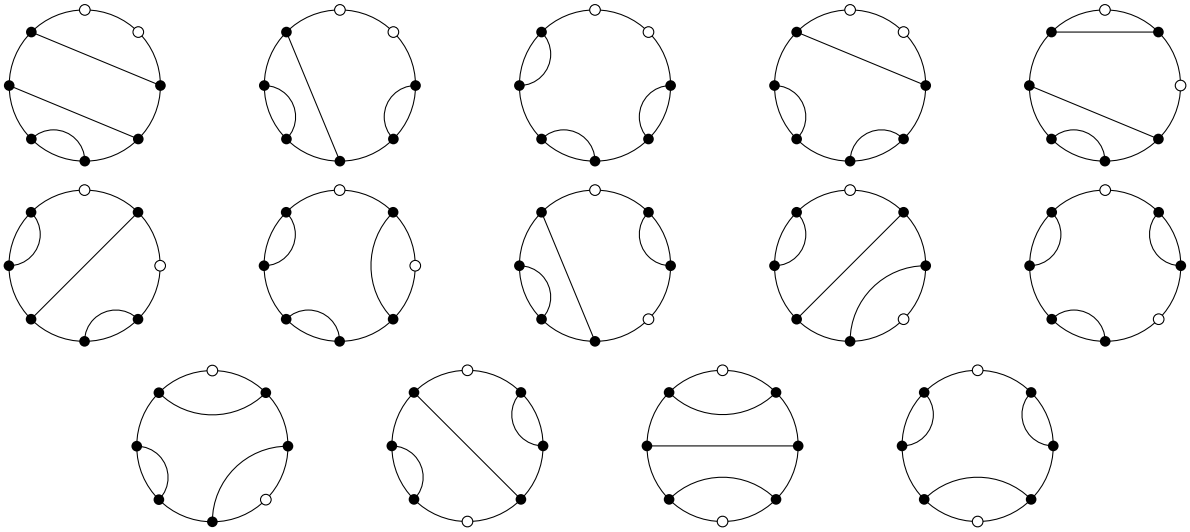

Figure 6. The enumeration of sl_2-webs with 6 black and 2 white vertices.

Figure 7 shows the non-crossing matchings with 10 black boundary vertices, which also have listed in [16, Appendix], totaling six types up to dihedral symmetry.

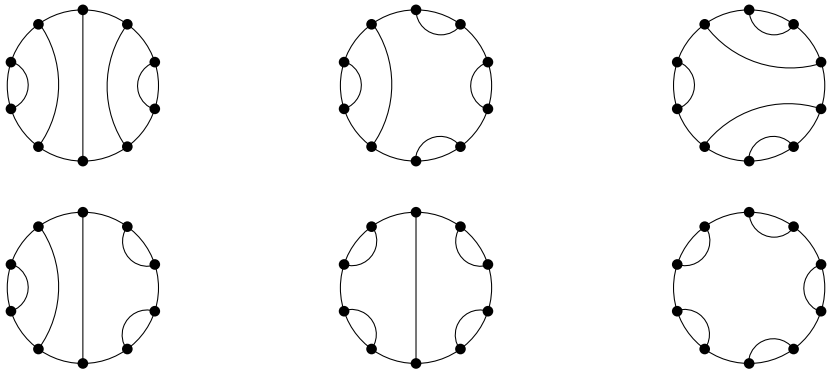

Figure 7. The enumeration of sl_2-webs with 10 black vertices.

4.2. Two examples of webs corresponding to quadratic differences

In this section, we present two representative examples illustrating how the method of compatibility and the method of diagram produce the same sl_2-web for a rank 2 cluster variable.

The first example essentially involves embedding a cluster variable of $\mathrm{Gr}(5,9)$ into $\mathrm{Gr}(5,10)$ by setting $\lambda_i = 0$ for one $1 \leq i \leq 10$, which identifies $\mathrm{Gr}(5,9)$ as a cluster subalgebra of $\mathrm{Gr}(5,10)$. For convenience, the cluster polynomial corresponding to the tableau T is the polynomial $ch(T)$ given by Theorem 2.2, and the tenth boundary vertex is labeled by A when it appears in the subscripts.

Example 4.1. *For semi-standard Young tableau* $T_1 = \begin{array}{|c|c|}\hline 1&1\\\hline 2&5\\\hline 3&7\\\hline 4&8\\\hline 6&9\\\hline\end{array}$, $\lambda_{T_1} = \{2,1,\ldots,1,\ 0\}$, *and* $\mathrm{ch}(T_1) = P_{15678}P_{12349} - P_{15679}P_{12348} + P_{15689}P_{12347}$, *we denote the* 3 *monomials of* $\mathrm{ch}(T_1)$ *by* $P_1 = P_{15678}P_{12349}$, $P_2 = -P_{15679}P_{12348}$, *and* $P_3 = P_{15689}P_{12347}$.

For P_1, $I\backslash J = \{5,6,7,8\}$, *and* $J\backslash I = \{2,3,4,9\}$, *so every web compatible with this polynomial appears in Figure 5. (Recall that Figure 5 lists mirror images separately, which is intended to facilitate this look-up.). Similarly, compatible webs of* P_2 *and* P_3 *appear there.*

In Figure 8, we list the webs compatible with P_1 *(*W_1*),* P_2 *(*W_1 *and* W_2*), and* P_3 *(*W_2 *and* W_3*). By Theorem 3.1, each quadratic monomial contributes the immanants of its compatible webs, so the contributions of* W_1 *and* W_2 *from* P_1 *and* P_2 *cancel, leaving only the immanant of* W_3 *in* $ch(T_1)$*. Thus we identify* W_3 *as the web corresponding to* T_1.

The web obtained above is derived using the method of compatibility. In addition, we can obtain another web (which turns out to be the same web) through the method of diagram.

Figure 9 depicts this process. First, the two 1*s in the first row are relabeled* 1 *(left) and* 2 *(right),and all other i are relabeled* $i+1$. *Then by Definition 5, there are* 5 *arcs in the diagram:* $\{1,2\}$, $\{5,6\}$, $\{8,7\}$, $\{4,9\}$, *and* $\{3,10\}$. *After drawing the web with* 10 *black vertices, we collapse boundary vertices* 1 *and* 2 *to a white sink vertex.*

Consequently, application of both the method of compatibility and the cup-diagram method produces the web corresponding to this cluster variable. The two webs thus obtained are identical.

Remark 4.2. By the Plücker relation for $(I,J) = (\{1,2,3,4\},\{1,5,6,7,8,9\})$,

$$P_{12345}P_{16789} - P_{12346}P_{15789} + P_{12347}P_{15689} - P_{12348}P_{15679} + P_{12349}P_{15678} = 0,$$

we may equivalently rewrite

$$ch(T_1) = P_{12346}P_{15789} - P_{12345}P_{16789}.$$

as it appears in Section 5, the polynomial P_9. But we keep the three-term expansion here because it makes the cancellation mechanism in the compatibility method more transparent.

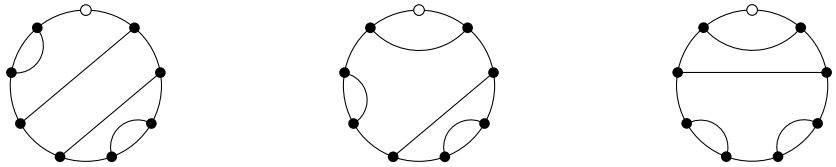

Figure 8. The non-crossing webs compatible with $P_1(W_1)$, $P_2(W_1$ and $W_2)$, and $P_3(W_2$ and $W_3)$ in $\mathrm{ch}(T_1)$. The web corresponding to $\mathrm{ch}(T_1)$ is W_3.

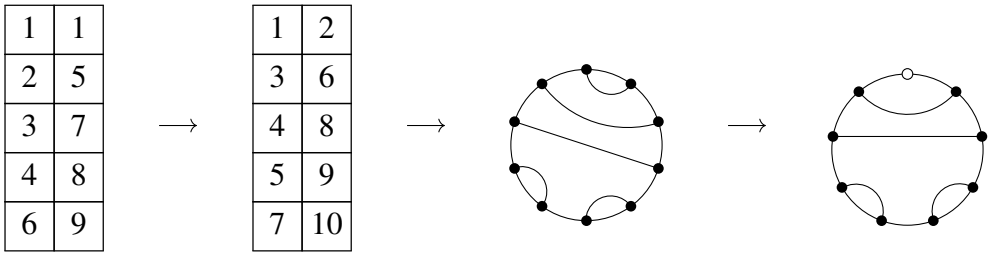

Figure 9. The procedure from semi-standard Young tableau to web by the method of diagram.

Example 4.3. *For standard Young tableau* $T_2 = \begin{array}{|c|c|}\hline 1&4\\\hline 2&5\\\hline 3&8\\\hline 6&9\\\hline 7&10\\\hline\end{array}$, $\lambda_{T_2} = \{1, 1, \ldots, 1, 1\}$, *and* $\mathrm{ch}(T_2) = P_{12345}P_{6789A} - P_{12346}P_{5789A} + P_{12347}P_{5689A} + P_{12356}P_{4789A} - P_{12357}P_{4689A} + P_{12367}P_{4589A}$. *Similarly to* T_1, *the polynomial is divided into 6 monomials which are denoted by* $P_i (i = 1, 2, \ldots, 6)$.

For each P_i, $I\backslash J = I$, *and* $J\backslash I = J$, *so its compatible webs are dihedral translates of the webs shown in Figure 7.*

In Figure 10, we list the webs compatible with P_1 *(*W_1*),* P_2 *(*W_1 *and* W_6*),* P_3 *(*W_4 *and* W_6*),* P_4 *(*W_5 *and* W_6*),* P_5 *(*W_1*,* W_2*,* W_4*,* W_5 *and* W_6*), and* P_6 *(*W_1*,* W_2 *and* W_3*). Thus, we can identify the web* W_3 *as the web corresponding to* T_2.

The web obtained above is derived using the method of compatibility. In addition, we can obtain another web (which turns to be the same web) through the method of diagram.

Figure 11 depicts this process. Since T_2 *itself is a standard Young tableau, it can be directly transformed into cup diagrams, whose arcs are* $\{3, 4\}$, $\{2, 5\}$, $\{7, 8\}$, $\{6, 9\}$, *and* $\{1, 10\}$.

Consequently, application of both the method of compatibility and the cup-diagram method produces the web corresponding to this cluster variable. The two webs thus obtained are identical.

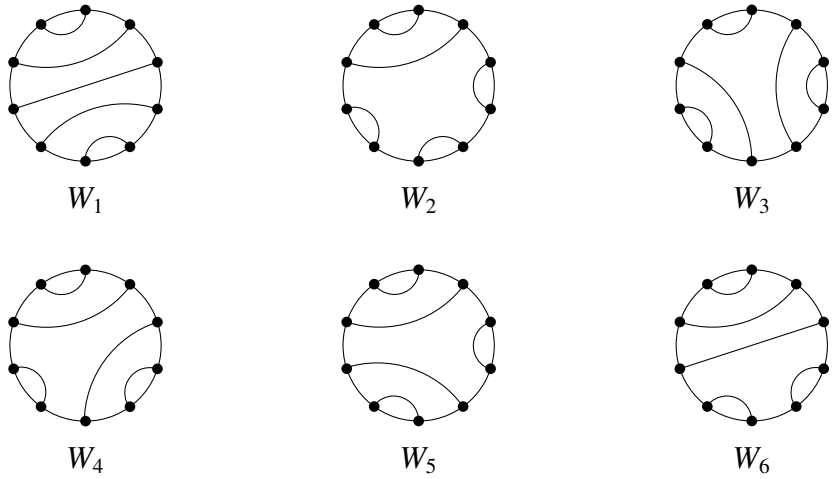

Figure 10. The non-crossing webs compatible with $P_1(W_1)$, $P_2(W_1$ and $W_6)$, $P_3(W_4$ and $W_6)$, $P_4(W_5$ and $W_6)$, $P_5(W_1, W_2, W_4, W_5$ and $W_6)$, and $P_6(W_1, W_2$ and $W_3)$ in ch(T_2). The web correspond to ch(T_2) is W_3.

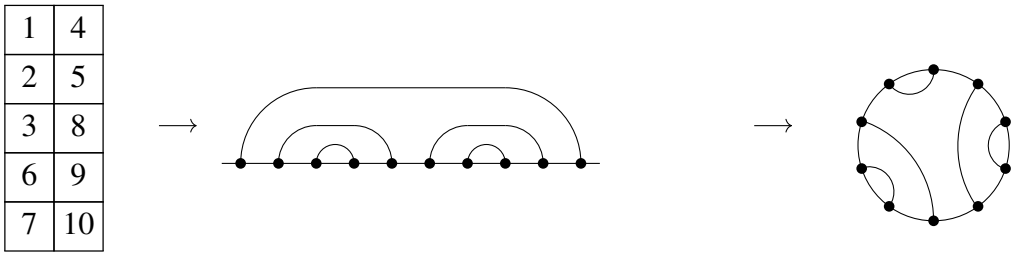

Figure 11. The procedure from standard Young tableau to web by the method of diagram.

4.3. The webs of rank 2 cluster variables in Gr(5,9)

For all rank 2 cluster variables of Gr$(5, 9)$ appearing in the computational enumeration, this section presents their corresponding sl_2-webs.

Since Gr$(5, 9) \cong$ Gr$(4, 9)$, we follow the computational enumeration in [20] and take their list of 576 rank 2 cluster variables in Gr$(5, 9)$ as input data. The dihedral group acts on Gr$(5, 9)$ by cyclic shifts and reflections of the boundary labels, and we use this symmetry to organize the computation into dihedral orbits.

Within this enumerated list, the variables fall into two types: 504 involve only 8 labels, while 72 involve all 9 labels. The 504 variables using only 8 labels correspond (via the natural identification Gr$(5, 8) \cong$ Gr$(3, 8)$) to the 56 rank 2 cluster variables in Gr$(5, 8)$.

This reduction is justified because the formula for ch(T) in Theorem 2.2 depends only on the relative order of the labels that actually appear in T (together with the fixed column order). Hence, whenever T involves exactly eight distinct labels, we may relabel them in increasing order by $1, 2, \ldots, 8$; under this order-preserving relabeling, the polynomial ch(T) is carried to the corresponding polynomial in $\mathbb{C}$[Gr$(5, 8)$], and conversely the original ch(T) is recovered by undoing the same relabeling on Plücker indices.

Consequently, for the purpose of computing the associated webs for all variables appearing in the enumeration, it suffices to compute the 56 variables in Gr$(5, 8)$ and the 72 variables in Gr$(5, 9)$ involving

all 9 labels.

Lemma 4.4. *For any rank* 2 *cluster variable in* Gr(5, 8) *appearing in Table 1, the web corresponding to it in both methods is a dihedral translation of the* 6 *webs in Figure 12.*

Proof. Using a method similar to Example 4.1, we verify the 56 rank 2 cluster variables of Gr(5, 8) using the two different methods. These variables correspond to dihedral translates of the 6 sl_2-webs shown in Figure 12, and the specific correspondences are listed in Table 1.

Since Gr(5, 8) ≅ Gr(3, 8), the cluster variables of Gr(5, 8) can be viewed as cluster variables in Gr(3, 8). Consequently, Figure 12 can be obtained more directly by inserting two white vertices into the sl_2-webs corresponding to cluster variables in $\mathbb{C}$[Gr(3, 6)]. In fact, all of these diagrams appear in the first example of [16, Figure 3], but we discuss only the portion concerning cluster variables. □

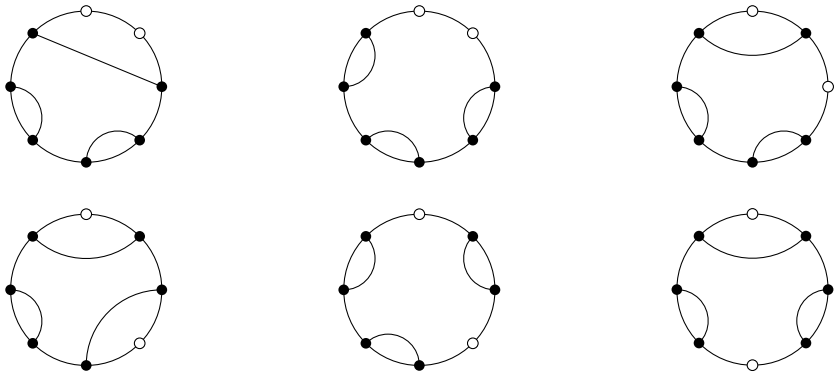

Figure 12. All webs corresponding to rank 2 cluster variables in Gr(5,8).

Lemma 4.5. *For any rank* 2 *cluster variable in* Gr(5, 9) *appearing in Table 2 with no isolated vertex (all* 9 *vertices appear in the cluster variable), the web corresponding to it in both methods is a dihedral translation of the* 5 *webs in Figure 13.*

Proof. Using a method similar to Example 4.1, we can calculate the 72 such rank 2 cluster variables of Gr(5, 9) using the two different methods. These variables correspond to dihedral translates of the 5 sl_2-webs shown in Figure 13, and the specific correspondences are listed in Table 2.

Similar to the proof of Lemma 4.4, Gr(5, 9) ≅ Gr(4, 9), the cluster variables of Gr(5, 9) can be viewed as cluster variables in Gr(4, 9). Consequently, Figure 13 can be obtained more directly by inserting a white vertex into the sl_2-webs corresponding to cluster variables in $\mathbb{C}$[Gr(4, 8)]. In fact, all of these diagrams appear in the second example of [16, Figure 3], but we discuss only the portion concerning cluster variables. □

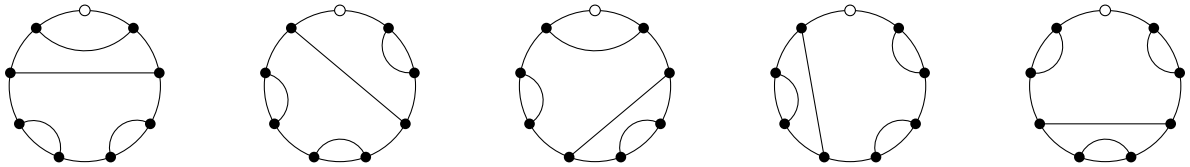

Figure 13. Webs corresponding to rank 2 cluster variables in Gr(5, 9) with no isolated vertices. In contrast to Figure 5, we list these representatives up to dihedral symmetry (cyclic shifts and reflections of the boundary labels), since such dihedral relabelings induce the corresponding relabeling of Plücker coordinates and hence carry the associated polynomials and tableau data to one another.

Theorem 4.6. *For all rank* 2 *cluster variables in* Gr(5, 9) *appearing in the computational enumeration, the web from the method of diagram is the same as the web from the method of compatibility.*

The lemmas and theorem above can be verified by the methods described in Section 3. In Section 5, some typical cluster variables and their corresponding webs are listed, and others are all dihedral translations of them.

Conjecture 4.7. *For any cluster variable written as both a Young tableau and a polynomial, the corresponding webs from the method of diagram and compatibility are the same.*

Conjecture 4.7 is stated in the sl_2-web setting used throughout this paper. For sl_3-webs, a natural analogue of the diagram side is available via the m-diagram constructions of [12, 13], which may be viewed as a direct extension of our cup-diagrams to the $3 \times n$ case and produce sl_3-webs. We do not attempt to formulate or verify the corresponding higher-rank compatibility procedure here. For general $r > 3$, we are not aware of a comparably explicit diagrammatic model attached to tableaux in the present context; nevertheless, it is tempting to expect that growth-type algorithms in [18] may provide a suitable framework for organizing such higher-rank structures.

Fraser et al. [16] records sl_2-web information related to certain quadratic elements of the dual canonical basis in Gr(3, 9), Gr(4, 8), and Gr(5, 10), which may be viewed as explicit data on the compatibility side; Elkin et al. [9] provides web-related computations for Gr(3, 8) via the twist map and dimer configuration; Banaian et al. [26] develops further higher-rank structures and examples for Gr(4, 12); and Fraser et al. [17] gives the universal form of webs and dual webs for the dual canonical basis in Gr($k, 2k$). On the other hand, ch(T) admits an explicit computable formula by [21, Theorem 5.8] (our Theorem 2.2). Hence these works supply a concrete source of comparison and evidence for Conjecture 4.7, namely that the diagram and compatibility procedures single out the same web.

Remark 4.8. Let $H(T)$ denote the element of the dual canonical basis in $\mathbb{C}[\mathrm{Gr}(k, n)]$ indexed by a semi-standard Young tableau T, as in Lam's work on cyclic Demazure modules and positroid varieties; see [19, §2, Theorem 1(ii) and Proposition 4]. These results imply that the degree-two component of $\mathbb{C}[\mathrm{Gr}(k, n)]$ admits a basis given by web (or Temperley–Lieb) immanants, and more precisely that, if $W[T]$ denotes the sl_2-web corresponding to T under the standard web–tableau correspondence in [21], then $H(T)$ is equal to the web immanant of $W[T]$.

Moreover, in [21] the authors attach to each semi-standard Young tableau T an element $ch(T) \in \mathbb{C}[\mathrm{Gr}(k, n)]$ and conjecture that the family $\{ch(T)\}$ forms the dual canonical basis. Our computations

in Section 5 can thus be interpreted as showing that, for the rank two cluster variables in Gr(5, 9) considered in this paper, the elements $ch(T)$ agree with the corresponding dual canonical basis elements $H(T)$ and hence with the immanants of the webs $W[T]$. In particular, Conjecture 4.7 may be reformulated as the statement that $ch(T) = H(T)$ whenever $ch(T)$ is a cluster variable. If one extends this statement to all semi-standard Young tableaux T, then, in view of the conjecture of [21] that the elements $ch(T)$ form the dual canonical basis, this extended version is essentially equivalent to the conjecture of [21].

We also note that it has now been proved that ch(T) is the dual canonical basis element indexed by T; see [27, Section 3.4]. Since the leading term of ch(T) is the standard monomial P_T, this identification matches the usual labeling of the dual canonical basis elements H(T) in Lam's notation. Consequently, Lam's Theorem 1(iv) in [19] implies that ch(T) (equivalently H(T)) is equivariant with respect to promotion and rotation. On the other hand, the behaviour under evacuation remains conjectural; see [27, Conjecture 7.9].

In fact, this conjecture is similar to [16, Observation 8.3], but the observation does not involve the case of $n \neq kr$.

5. Proof of Theorem 4.6

All sl_2-webs arising from the rank 2 cluster variables considered in this section occur among the webs listed in Figures 5 and 6. To choose explicit representatives, we fix a normalization for dihedral relabellings: We place a white boundary vertex at the top, so that $\lambda_1 = 2$, and in the cases with an isolated vertex we further normalize by allowing only λ_9 to be zero. This normalization is used only to select orbit representatives for presentation, and not as a restriction on which variables are computed.

We followed the computational procedure of [20] to reproduce the list of 576 rank 2 cluster variables in $\mathbb{C}[\mathrm{Gr}(5, 9)]$ used in this section. As in the rest of the paper, we take this enumeration as input data and do not claim an independent proof of its completeness.

For each of the 576 variables, we computed the associated sl_2-web using the method of compatibility and the method of diagram, and we verified that the two resulting webs agree. This completes the proof of Theorem 4.6 for all variables in the reproduced list.

To organize and present these fully checked data, we classify the variables by rotation (cyclic relabeling). On the tableau side, this corresponds to promotion (see [28]). In the 8-label case, under the normalization above, we obtain seven promotion representatives, denoted $P_1, \ldots, P_7$. Their polynomials are as follows (each is a difference of two monomials):

- $P_1 = P_{12356}P_{12478} - P_{12456}P_{12378}$
- $P_2 = P_{12367}P_{12458} - P_{12345}P_{12678}$
- $P_3 = P_{12346}P_{13578} - P_{12345}P_{13678}$
- $P_4 = P_{12368}P_{13457} - P_{12378}P_{13456}$
- $P_5 = P_{13458}P_{12467} - P_{14678}P_{12345}$
- $P_6 = P_{14568}P_{12347} - P_{14567}P_{12348}$
- $P_7 = P_{12356}P_{14578} - P_{12345}P_{15678}$.

The corresponding tableaux, cluster polynomials, and webs are recorded in Table 1.

Table 1. The 7 webs corresponding to the rank 2 cluster variables in Gr(5, 8).

tableau	polynomial	web	tableau	polynomial	web
1 1 2 2 3 5 4 7 6 8	$+P_{12356}P_{12478}$ $-P_{12456}P_{12378}$	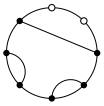	1 1 2 2 3 4 5 6 7 8	$+P_{12367}P_{12458}$ $-P_{12345}P_{12678}$	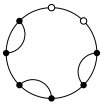
1 1 2 3 3 5 4 7 6 8	$+P_{12346}P_{13578}$ $-P_{12345}P_{13678}$	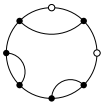	1 1 2 3 3 4 5 6 7 8	$+P_{12368}P_{13457}$ $-P_{12378}P_{13456}$	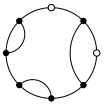
1 1 2 3 4 4 5 6 7 8	$+P_{13458}P_{12467}$ $-P_{14678}P_{12345}$	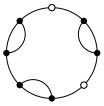	1 1 2 4 3 5 4 7 6 8	$+P_{14568}P_{12347}$ $-P_{14567}P_{12348}$	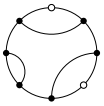
1 1 2 3 4 5 5 6 7 8	$+P_{12356}P_{14578}$ $-P_{12345}P_{15678}$	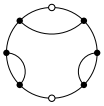			

In the 9-label case, under the same normalization, we obtain eight promotion representatives, denoted $P_8, \ldots, P_{15}$. Their polynomials are as follows:

- $P_8 = P_{12346}P_{15789} - P_{12345}P_{16789}$
- $P_9 = P_{13457}P_{12689} - P_{13456}P_{12789}$
- $P_{10} = P_{14678}P_{12359} - P_{15678}P_{12349}$
- $P_{11} = P_{12348}P_{15679} - P_{12349}P_{15678}$
- $P_{12} = P_{12456}P_{13789} - P_{13456}P_{12789}$
- $P_{13} = P_{13567}P_{12489} - P_{14567}P_{12389}$
- $P_{14} = P_{14568}P_{12379} - P_{14567}P_{12389}$
- $P_{15} = P_{13459}P_{12678} - P_{12345}P_{16789}$

The corresponding tableaux, cluster polynomials, and webs are recorded in Table 2. Altogether, this yields 15 promotion representatives, which serve as explicit representatives for organizing and locating all 576 variables in the reproduced list under rotation (promotion).

Table 2. The 8 webs corresponding to the rank 2 cluster variables in Gr(5, 9).

tableau	polynomial	web	tableau	polynomial	web
1 1 2 5 3 7 4 8 6 9	$+P_{12346}P_{15789}$ $-P_{12345}P_{16789}$	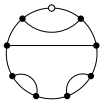	1 1 2 3 4 6 5 8 7 9	$+P_{13457}P_{12689}$ $-P_{13456}P_{12789}$	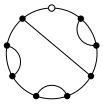
1 1 2 4 3 6 5 7 8 9	$+P_{14678}P_{12359}$ $-P_{15678}P_{12349}$	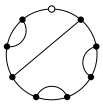	1 1 2 5 3 6 4 8 7 9	$+P_{12348}P_{15679}$ $-P_{12349}P_{15678}$	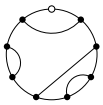
1 1 2 4 3 7 5 8 6 9	$+P_{12456}P_{13789}$ $-P_{13456}P_{12789}$	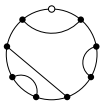	1 1 2 3 4 5 6 8 7 9	$+P_{13567}P_{12489}$ $-P_{14567}P_{12389}$	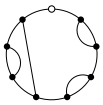
1 1 2 4 3 5 6 7 8 9	$+P_{14568}P_{12379}$ $-P_{14567}P_{12389}$	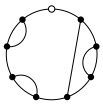	1 1 2 3 4 6 5 7 8 9	$+P_{13459}P_{12678}$ $-P_{12345}P_{16789}$	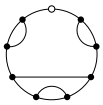

Next we consider the reflection ρ (which corresponds to evacuation on the tableau side; see [28]). We emphasize that the following consolidation into "dihedral types" is not obtained by an inductive guess: it is obtained by first computing, for every one of the 576 variables, the two webs produced by the compatibility method and the diagram method and checking that they agree, and then organizing these verified outputs under the actions of rotation and reflection. The resulting organization shows that, in the 8-label case, the seven promotion representatives consolidate into six dihedral types under ρ; in the 9-label case, the eight promotion representatives consolidate into five dihedral types under ρ. Therefore, after taking both rotation and reflection into account, we obtain 11 distinct dihedral representatives. Explicitly, they are P_1, P_2, P_3, P_5, P_6, P_7, P_8, P_9, P_{11}, P_{13}, P_{15}.

On the other hand, [27, Conjecture 7.9] predicts a corresponding symmetry for ch(T) under evacuation. The 11 dihedral types obtained in the rank two case of Gr(5, 9) are consistent with the symmetry pattern predicted by that conjecture; thus, our results may be viewed as an explicit check of the conjecture in this concrete setting.

Finally, we reiterate that we do not claim an independent proof of completeness of the reproduced enumeration.

6. Conclusions

In this paper, we studied rank 2 cluster variables in $\mathbb{C}$[Gr(5, 9)] from two complementary viewpoints: the compatibility method for quadratic Plücker polynomials and the diagram method arising from semi-standard Young tableaux. Taking the computational enumeration of 576 rank 2 cluster variables

in Gr(5, 9) from [20] as input data, we computed the associated sl_2-webs and verified that, for every variable in this reproduced list, the web obtained from the diagram method coincides with the web obtained from the compatibility method.

Up to dihedral symmetry, these rank 2 cluster variables give rise to 11 distinct sl_2-webs. This provides explicit evidence that, in the rank 2 setting of Gr(5, 9), the tableau-theoretic and compatibility-theoretic descriptions select the same web. In particular, our computations support Conjecture 4.7, which predicts that whenever a cluster variable is written both as a Young tableau and as a polynomial, the corresponding webs from the two methods are identical.

Our results also suggest several directions for further study. A natural next step is to investigate analogous questions for sl_3-webs, where m-diagram models are available, and more generally to seek a higher-rank framework relating tableau constructions, compatibility, and dual canonical basis phenomena in a uniform way. It would also be desirable to replace the computational input used here by a more conceptual structural explanation for why the two procedures must agree.

Author contributions

Rui Zhi Tang: Computation, formal analysis, investigation, and writing—original draft preparation; Jin Xing Zhao: Validation and writing—review and editing. All authors have read and agreed to the published version of the manuscript.

Use of Generative-AI tools declaration

The authors declare they have not used Artificial Intelligence (AI) tools in the creation of this article.

Acknowledgments

This work was supported by the National Natural Science Foundation of China (No. 12161062), the Inner Mongolia Natural Science Foundation (No. 2025MS01022), the Hohhot Science and Technology Program (No. 2025-Gui-Ji-59), and the China Postdoctoral Science Foundation (No. 2025MD774102). The authors would like to thank Professor W. T. Zhang and Professor J. R. Li for their helpful discussions and valuable suggestions.

Conflict of interest

The authors declare no conflict of interest in this paper.

References

1. S. Fomin, A. Zelevinsky, Cluster algebras I: Foundations, *J. Amer. Math. Soc.,* **15** (2002), 497–529. https://doi.org/10.1016/S0950-7051(02)00058-8
2. J. S. Scott, Grassmannians and cluster algebras, *Proc. Lond. Math. Soc.,* **92** (2006), 345–380. https://doi.org/10.1112/S0024611505015571

3. A. Postnikov, Total positivity, Grassmannians, and networks, *arXiv preprint*, 2006. Available from: https://arxiv.org/abs/math/0609764.
4. K. Talaska, A formula for Plücker coordinates associated with a planar network, *Int. Math. Res. Not.,* **2008** (2008), rnn081. http://dx.doi.org/10.1093/imrn/rnn081
5. G. Muller, D. Speyer, The twist for positroid varieties, *Proc. Lond. Math. Soc.,* **115** (2016). http://dx.doi.org/10.1112/plms.12056
6. R. J. Marsh, J. S. Scott, Twists of Plücker coordinates as dimer partition functions, *Commun. Math. Phys.,* **341** (2016), 821–884. http://dx.doi.org/10.1007/s00220-015-2493-7
7. A. Berenstein, S. Fomin, A. Zelevinsky, Parametrizations of canonical bases and totally positive matrices, *Adv. Math.,* **122** (1996), 49–149. https://doi.org/10.1006/aima.1996.0057
8. T. Lam, Dimers, webs, and positroids, *J. Lond. Math. Soc.,* **92** (2015), 633–656. https://doi.org/10.1112/jlms/jdv039
9. M. Elkin, G. Musiker, K. Wright, Twists of Gr(3,n) cluster variables as double and triple dimer partition functions, *arXiv preprint*, 2024. Available from: https://arxiv.org/abs/2305.15531.
10. B. W. Westbury, The representation theory of the Temperley–Lieb algebras, *Math. Z.,* **219** (1995), 539–565. Available from: https://api.semanticscholar.org/CorpusID:125073960.
11. F. Y. Fung, On the topology of components of some Springer fibers and their relation to Kazhdan–Lusztig theory, *Adv. Math.,* **178** (2003), 244–276. http://dx.doi.org/10.1016/S0001-8708(02)00072-5
12. J. Tymoczko, A simple bijection between standard $3 \times$ n tableaux and irreducible webs for $\mathfrak{sl}(3)$, *J. Algebraic Combin.,* **35** (2012), 611–632. https://doi.org/10.1159/000233214
13. H. M. Russell, An explicit bijection between semistandard tableaux and non-elliptic sl_3 webs, *J. Algebraic Combin.,* **38** (2013), 851–862. http://dx.doi.org/10.1007/s10801-013-0428-y
14. G. Kuperberg, Spiders for rank 2 Lie algebras, *Commun. Math. Phys.,* **180** (1996), 109–151. https://doi.org/10.1007/BF02101184
15. S. Fomin, P. Pylyavskyy, Tensor diagrams and cluster algebras, *Adv. Math.,* **300** (2016), 717–787. https://doi.org/10.1016/j.aim.2016.03.030
16. C. Fraser, T. Lam, I. Le, From dimers to webs, *Trans. Amer. Math. Soc.,* **371** (2019), 6087–6124. https://doi.org/10.1090/tran/7641
17. C. Fraser, Webs and canonical bases in degree two, *arXiv preprint*, 2023. Available from: https://arxiv.org/abs/2202.01310.
18. C. Gaetz, O. Pechenik, S. Pfannerer, J. Striker, J. P. Swanson, Rotation-invariant web bases from hourglass plabic graphs, *arXiv preprint*, 2023. Available from: https://arxiv.org/abs/2306.12501.
19. T. Lam, Cyclic Demazure modules and Positroid varieties, *Electron. J. Combin.,* **26** (2019), P2.28. http://dx.doi.org/10.37236/8383
20. M. W. Cheung, P. P. Dechant, Y. H. He, E. Heyes, E. Hirst, J. R. Li, Clustering cluster algebras with clusters, *Adv. Theor. Math. Phys.,* **27** (2023). http://dx.doi.org/10.4310/ATMP.2023.v27.n3.a5

21. W. Chang, B. Duan, C. Fraser, J. R. Li, Quantum affine algebras and Grassmannians, *Math. Z.,* **296** (2020), 1539–1583. https://doi.org/10.1007/s00209-020-02496-7

22. S. Fomin, L. Williams, A. Zelevinsky, *Introduction to Cluster algebras. Chapter 6*, 2021. Available from: `https://arxiv.org/abs/2008.09189`.

23. D. Kim, Graphical calculus on representations of quantum Lie algebras, *arXiv preprint*, 2003. Available from: `https://arxiv.org/abs/math/0310143`.

24. S. Morrison, A diagrammatic category for the representation theory of $U_q(\mathfrak{sl}_n)$, *arXiv preprint*, 2007. Available from: `https://arxiv.org/abs/0704.1503`.

25. S. Cautis, J. Kamnitzer, S. Morrison, Webs and quantum skew Howe duality, *Math. Ann.,* **360** (2014), 351–390. http://dx.doi.org/10.1007/s00208-013-0984-4

26. E. Banaian, E. Catania, C. Gaetz, M. Moore, G. Musiker, K. Wright, Twists, higher dimer covers, and web duality for Grassmannian cluster algebras, *arXiv preprint*, 2025. Available from: `https://arxiv.org/abs/2507.15211`.

27. J. Drummond, O. Gurdogan, J. R. Li, Tropical symmetries of cluster algebras, *arXiv preprint*, 2026. Available from: `https://arxiv.org/abs/2601.19779`.

28. R. P. Stanley, Promotion and evacuation, *Electron. J. Combin.,* **15** (2008), R00.

AIMS Press